Extreme Mechanics Letters 1 (2014) 90–96

Contents lists available at ScienceDirect

Extreme Mechanics Letters

journal homepage: www.elsevier.com/locate/eml

Fiber-reinforced tough hydrogels

Widusha R.K. Illeperuma [a], Jeong-Yun Sun [b], Zhigang Suo [a,*], Joost J. Vlassak [a,*]

[a] School of Engineering and Applied Sciences, Harvard University, Cambridge, MA 02138, USA

[b] Department of Material Science and Engineering, Seoul National University, Seoul 151-744, South Korea

ARTICLE INFO

Article history:
Received 1 September 2014
Received in revised form 5 November 2014
Accepted 8 November 2014
Available online 26 November 2014

Keywords:
Tough hydrogel
Hydrogel composite
Fiber pullout

ABSTRACT

Using strong fibers to reinforce a hydrogel is highly desirable but difficult. Such a composite would combine the attributes of a solid that provides strength and a liquid that transports matter. Most hydrogels, however, are brittle, allowing the fibers to cut through the hydrogel when the composite is loaded. Here we circumvent this problem by using a recently developed tough hydrogel. We fabricate a composite using an alginate–polyacrylamide hydrogel reinforced with a random network of stainless steel fibers. Because the hydrogel is tough, the composite does not fail by the fibers cutting the hydrogel; instead, it fails by the fibers pulling out of the hydrogel against friction. Both stiffness and strength can be increased significantly by adding fibers to the hydrogel. Before failure the composite dissipates a significant amount of energy, at a tunable level of stress, attaining large deformation. Potential applications of tough hydrogel composites include energy-absorbing helmets, tendon repair surgery, and stretchable biometric sensors.

1. Introduction

Hydrogels are soft materials that consist of cross-linked networks of hydrophilic polymer chains dispersed in water. They have many applications including scaffolds in tissue engineering [1], carriers for drug delivery [2], and valves for microfluidic devices [3]. Many applications of hydrogels rely on the combined attributes of a solid that provides strength and a liquid that transports matter. Most existing hydrogels, however, are brittle, with fracture energies on the order of 10 J/m^2 [4,5]. This limits their use in structural applications where they are subject to mechanical loading. This problem could be circumvented by reinforcing the hydrogels with fibers to improve their mechanical behavior [6]. This effort is hampered, however, by the low toughness of hydrogels: as the composite is loaded, the fibers cut through the hydrogel matrix, destroying the synergy between fibers and matrix, and leading to rapid failure of the composite. A hydrogel-based composite is only effective if the hydrogel matrix is tough enough to resist the fibers cutting through the matrix. Cartilage is one example of such a composite taken from nature: cartilage consists of a collagen fiber-reinforced proteoglycan gel. It contains more than 70% water, but is remarkably stiff and tough [7,4]. It comes as no surprise, then, that hydrogel-based composites are being actively explored for use as synthetic tissues and in biocompatible products [8–15].

Many attempts have been made to improve the toughness of hydrogels [12,14–17]. Double-network hydrogels were the first class of hydrogels to exhibit significant fracture toughness, with fracture energies in the range of 100–1000 $J\,m^{-2}$ [14]. Recently, we developed a new group of hybrid hydrogels synthesized from polymers that form networks with covalent and ionic cross-links, and that have an extraordinary combination of toughness and stretchability [18]. These hybrid gels consist of a covalently cross-linked polyacrylamide (PAAm) network and an ionically

* Corresponding authors.
E-mail addresses: suo@seas.harvard.edu (Z. Suo), vlassak@seas.harvard.edu (J.J. Vlassak).

http://dx.doi.org/10.1016/j.eml.2014.11.001
2352-4316/

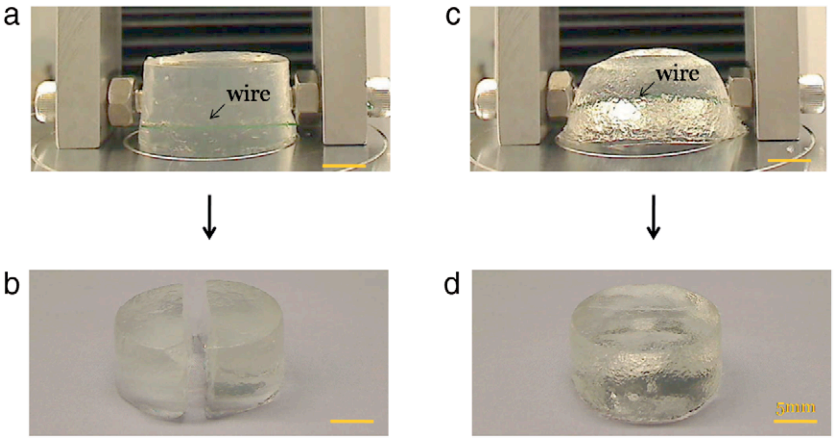

Fig. 1. Wire cutting tests for a brittle (a, b) and a tough hydrogel (c, d). (a) Alginate hydrogel being cut by a steel wire. (b) The cut sample is turned 90° and the two pieces are separated to show the cut. (c) Alginate–polyacrylamide hybrid hydrogel deforms, but resists cutting. (d) The sample recovers its original shape when the wire is removed.

cross-linked alginate network, and can attain fracture energies as large as 9000 J m^{-2}. The need for a tough composite matrix is illustrated graphically in Fig. 1, where we use a metal wire to cut through two different types of hydrogels, a standard technique for measuring the fracture toughness of food and soft gels [19,20]. Two examples are shown: (1) a brittle alginate gel and (2) a tough alginate–polyacrylamide hybrid hydrogel. The difference between the gels is obvious. The alginate gel is readily cut by the wire; the hybrid gel deforms elastically, but resists being cut. Thus an alginate matrix would result in a composite with poor mechanical properties. The hybrid gel, on the other hand, would make a very good matrix in a fiber-reinforced composite. Such a composite would have significantly better stiffness and strength than the hybrid hydrogel, and could be used in structural applications. Lin et al. [12] have investigated the toughening mechanism of alginate–polyacrylamide hydrogels reinforced by a stretchy fiber mesh fabricated from thermoplastic polymers. When a notched sample of such a composite is deformed, the hydrogel matrix maintains the integrity of the sample, while fracture of the fibers in the bridging zone dissipates mechanical energy.

In this study we investigate the mechanical behavior of composites that consist of a tough alginate–polyacrylamide hydrogel matrix reinforced with a random network of stiff fibers, for which we conveniently use stainless steel wool. Steel wool fibers are strong and can easily create a random continuous fiber network—they have been used for this purpose in a number of applications [21,22]. We evaluate the stress–strain curves of the fiber-reinforced gels and evaluate the mechanism by which they fail.

2. Experimental details

2.1. Synthesis of fiber reinforced hydrogels

Powders of alginate (FMC Biopolymer, LF 20/40) and acrylamide (Sigma, A8887) were dissolved in deionized water. After the powders were fully dissolved, the solution was held at 35 °C for 1 h. Weights of alginate and acrylamide were fixed at 1:6, and the water content was fixed at 86 wt%. Ammonium persulfate (AP; Sigma, A9164), 0.0017 times the weight of acrylamide, was added as a photo initiator for the acrylamide polymerization process. N,N-methylenebisacrylamide (MBAA; Sigma, M7279), 0.0006 times the weight of the acrylamide, was added as the cross-linker for the acrylamide. N,N,N′,N′-tetramethylethylenediamine (TEMED; Sigma, T7024), 0.0025 times the weight of acrylamide, was added as the cross-linking accelerator for the polyacrylamide. Calcium sulfate slurry ($CaSO_4 \bullet 2H_2O$; Sigma, 31 221), 0.1328 times the weight of alginate, was added as the ionic cross-linker for alginate. Stainless steel wool (Type 316, fine, McMaster-Carr 7364T74) with an average cross-sectional area of the fibers of $\sim$80 μm $\times$ 70 μm was chosen to provide the reinforcing fibers. The fibers in this type of steel wool are arbitrarily oriented and have lengths that exceed the sample dimensions. After the wool was distributed evenly inside dumbbell-shaped molds, the gel solution was poured into the molds and covered with a glass plate. Before casting the gel solution, the steel wool was thoroughly wetted with the solution to reduce the formation of bubbles inside the samples. The composite samples were then cured at room temperature by exposing them for eight minutes to ultraviolet light with a wavelength of 350 nm (OAI LS 30 UV flood exposure system, 1.92 W/cm^2 power density). The samples were kept in a sealed container at room temperature for one day to ensure complete reaction. The weight fraction of steel wool in the composite hybrid gels was varied from 0 to 12 wt%.

2.2. Wire cutting test

Hydrogel samples with a diameter of 35 mm and a thickness of 17 mm were fabricated from an unreinforced alginate–polyacrylamide hybrid hydrogel and an alginate hydrogel (Fig. 1). Wire cutting tests were performed in air, at room temperature, using a tensile tester (Instron model 3342) with a 1000 N load cell. A 580 μm diameter steel wire was pulled through the specimen at a displacement rate 10 mm/min.

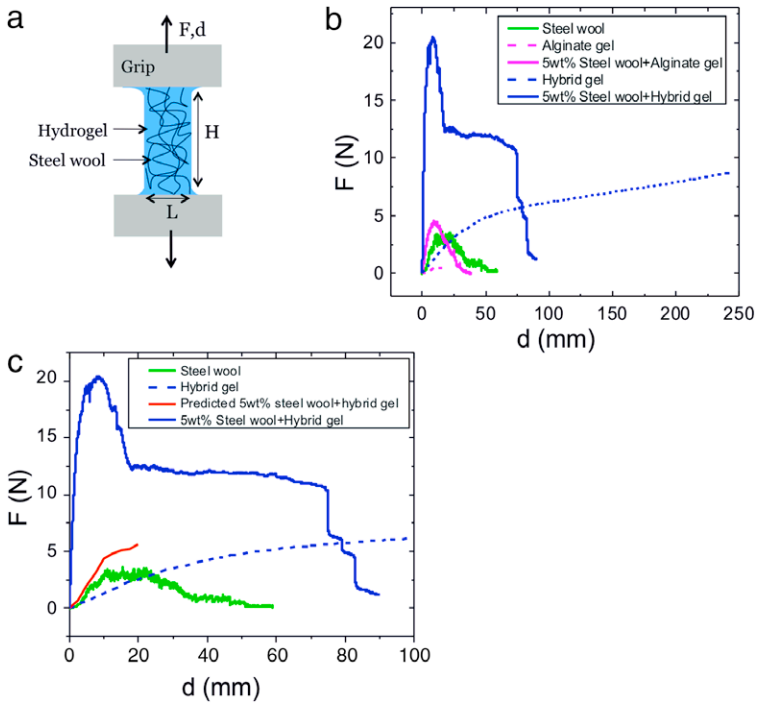

Fig. 2. Tensile tests of hydrogel composites. (a) Schematic of the tensile test samples of the fiber-reinforced hydrogels. Steel fibers form a random network throughout the entire sample. (b) Force–displacement curves for a fiber-reinforced hybrid hydrogel and a fiber-reinforced alginate hydrogel, compared with similar curves for steel wool and unreinforced hydrogels. (c) Force–displacement curve of hybrid hydrogel composite is predicted from hydrogel and steel wool at small displacements and compared with the experimental composite curve.

2.3. Tensile test

Tensile experiments were performed using the dumbbell-shaped samples. The gauge sections of the samples were 35 mm long, 15 mm wide, and 3 mm thick (Fig. 2(a)). The wide sections of the samples were glued between two acrylic plates of dimensions $10 \times 20 \times 3$ mm^3 using super glue (VWR, 500031-578) and the acrylic plate/gel sandwiches were inserted into the grips of the tensile tester. Measurements were performed at room temperature in air using a 1000 N load cell. The force–displacement curves were measured at a displacement rate of 10 mm/min. Tests were performed until rupture of the samples. The force–extension curve for steel wool was measured by performing measurements on the same amount of steel wool, randomly distributed in the same volume as the composite samples. Five experiments were performed per condition.

2.4. Fiber pullout test

The friction between the hydrogel matrix and the stainless steel fibers was measured using a fiber pullout test. A long fiber was embedded inside an alginate–polyacrylamide hydrogel during synthesis of the gel, such that a significant length of the fiber extended outside the gel on both sides of the sample. The samples had a height of 75 mm, width of 15 mm, and thickness of 3 mm. Fiber dimensions were measured at three locations along the length of each fiber by means of optical microscopy. The samples were mounted in the tensile tester and one end of the fiber was attached to the grip of the tensile tester. Pullout tests were performed in air, at room temperature, using a 1000 N load cell. Force–displacement curves were measured at a displacement rate of 10 mm/min. Tests were performed on five different samples.

3. Results and discussion

Fig. 2(b) shows the force–displacement curves for two different composites, a fiber-reinforced alginate–polyacrylamide hybrid gel and a fiber-reinforced alginate gel, along with the force–displacement curves of the various components that make up the composites. Both composites have the same weight fraction of stainless steel fibers. The pure alginate hydrogel is very weak and can sustain very small loads and displacements only. The pure hybrid hydrogel, in contrast, is very stretchable and can sustain much higher forces, but is quite compliant. The steel wool sample has poor mechanical properties and the sample essentially disintegrates during the test. The force–displacement curve of the alginate composite is not much different from that of the steel wool. Since the alginate is too weak to keep the fibers together, its behavior is almost completely controlled by the steel wool. The effect of fibers on the hybrid hydrogel, on the other hand, is substantial: it is much stronger and stiffer than the unreinforced hybrid gel, and it is significantly stronger than the reinforced alginate. Additionally, the force–displacement curve has a very different shape from both the steel wool and the hybrid gel; the force rises quickly, goes through a maximum, and then plateaus.

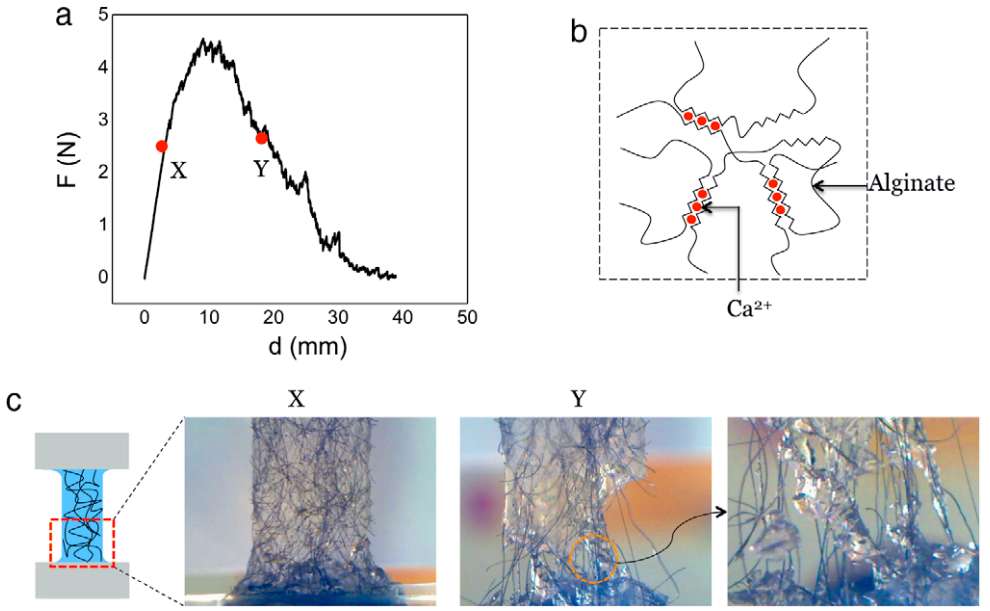

Fig. 3. Failure mechanism of a brittle and weak alginate hydrogel composite. (a) Force–displacement curve of an alginate hydrogel composite. (b) Schematic of the molecular structure of alginate hydrogel. (c) Photos at two stages during the tensile test. At small deformations (point X), the fibers are bonded to the matrix. After reaching a maximum force, the composite starts to fail by fibers cutting through the matrix (point Y).

To predict the force–displacement curve of the hydrogel composite at small displacements, the curves for steel wool and hydrogel are vertically added and plotted in Fig. 2(c). Evidently, the experimental curve does not follow the rule of mixtures based on the behavior of the constituents. This is understood as follows. The fibers in the steel wool are held together by entanglement only; they are not bonded in any way. During tensile testing, the fibers slide with respect to one another. Consequently, the tensile behavior is not representative of the mechanical behavior of the fibers; instead it is a measure for the frictional resistance encountered during fiber disentanglement. In contrast, the behavior of the fibers in the hydrogel is very different: the hydrogel matrix keeps the fibers in place and makes disentanglement very difficult. Disentanglement only occurs during the second stage after the fibers debond from the matrix. In other words, there is a strong synergistic effect when fibers and hydrogel are combined.

Fig. 3 shows the deformation of the reinforced alginate gel during the tensile test in more detail. The figure also shows a schematic of the molecular structure of the alginate chains with the Ca^{2+} crosslinks. As the load on the sample rises, the composite remains intact initially. When the load reaches a maximum, which is comparable to the maximum load supported by just the steel wool, the fibers start to disentangle, cutting through the alginate matrix in the process. This process continues with increased deformation until the fibers have completely shredded the matrix at the point of failure.

The tensile response of the fiber-reinforced alginate–polyacrylamide hydrogel is illustrated in detail in Fig. 4. The figure also shows a schematic of the molecular structure of the alginate–polyacrylamide hydrogel, with MBAA crosslinks in the polyacrylamide network and Ca^{2+} crosslinks in the alginate network. Initially, the fibers and matrix deform in concert. With continued deformation, the fibers rotate toward the loading direction and the load rises quickly to a value that is much larger than that predicted by the rule of mixtures applied to matrix and steel wool. At this point, the interface between fibers and matrix starts to debond and the load decreases until it reaches a plateau value characterized by continuous fiber sliding and pull out. During the fiber sliding stage, the matrix undergoes extensive deformation, but remains intact; there is no cutting by the fibers. Eventually the fiber network is ripped apart causing abrupt failure of the sample.

Because frictional sliding is an important aspect of the failure mechanism, single-fiber pullout tests were performed to investigate the interfacial properties (Fig. 5(a)). Fig. 5(b) shows a typical force–displacement curve for a fiber pullout experiment. The curves go through a maximum, which coincides with the failure of the interface between fiber and matrix. After debonding, the fiber pulls out of the matrix at a constant frictional force of approximately 0.155 ± 0.052 N. In the experiments, the peak load was difficult to reproduce, but the magnitude of the plateau force was very consistent. The average friction stress between fiber and matrix was calculated by dividing the frictional force by the total interfacial area between fiber and matrix, yielding a value of approximately 5 kPa. This result was used to estimate the energy dissipated by frictional sliding of the fibers. The total fiber length (6.78 m) was calculated from the mass of the fibers embedded in a typical sample (0.3 g), the density of steel (7.8 g/cm^3), and the average cross-sectional area ($80\ \mu m \times 70\ \mu m$) of the fibers. An upper bound for the energy dissipated in friction during the tensile test, can be found by multiplying the frictional force with the total fiber length, yielding a value of approximately 1.06 ± 0.35 J. The total energy dissipated during the tensile test can be calculated from the

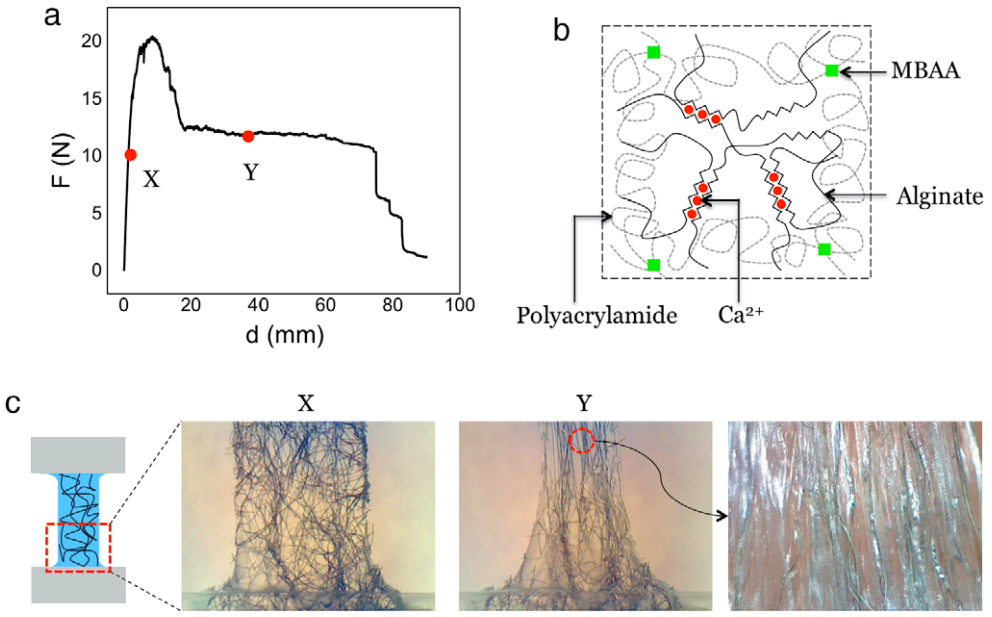

Fig. 4. Failure mechanism of a tough hybrid hydrogel composite. (a) Force–displacement curve of an alginate–polyacrylamide hydrogel composite. (b) Schematic of the molecular structure of alginate–polyacrylamide hydrogel. (c) Photos at two stages during the tensile test. At small displacements (point X), the fibers are bonded to the matrix. Fiber debonding is observed near the peak force. At larger displacements (point Y), the fibers slide through the matrix.

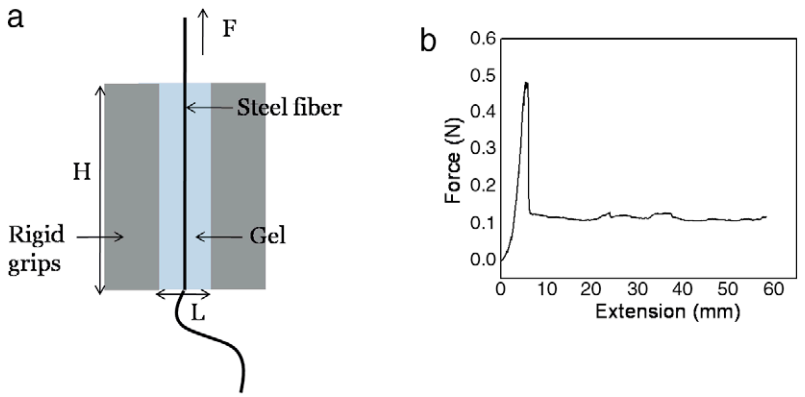

Fig. 5. Single fiber pull out test. (a) Schematic of the single fiber pullout test sample; (b) Force required to pull the fiber is recorded as a function of fiber extension.

force–displacement curve in Fig. 2(b), resulting in a value of 1.02 J. Part of this energy is dissipated in the deformation of the hydrogel matrix and this part can be estimated from the force–displacement curve of the hydrogel to yield 0.30 J. Thus the energy dissipated by fiber sliding is approximately 0.72 J, which compares favorably with the upper bound—approximately 70% of the total energy dissipation during the tensile test is associated with frictional losses.

Fig. 6(a) through (c) illustrate the effect of the volume fraction of the steel wool on the mechanical response of the composites. The nominal stress was obtained by dividing the force by the initial cross-sectional area of the sample; stretch was calculated by dividing the length of the deformed sample by its initial value. The tensile strength was defined as the maximum nominal stress supported by the composites. The elastic modulus was calculated from the slope of the stress–strain curves up to 5% strain. The fiber concentration was varied from 0 to 11.4 wt%. Without fiber reinforcement, the hybrid gel has a very large stretch to failure, but low stiffness and strength. Introducing the fibers reduces the stretchability of the gel, but increases the modulus and strength significantly. Evidently the weight fraction of the steel wool has a large effect on the stress–stretch curves: At low weight fraction, the response of the composite is dominated by the hydrogel and the stress–stretch curve is similar to that of a pure hydrogel. As the weight fraction is increased, the shape of the curve is altered and it develops a distinct peak followed by a plateau, associated with fiber debonding and sliding, respectively. At even higher weight fractions, the steel wool completely dominates the response, the plateau disappears, and the stress–stretch curve becomes similar to that of steel wool.

Synthesis of fiber-reinforced composites involves a large number of variables, including the type of fibers,

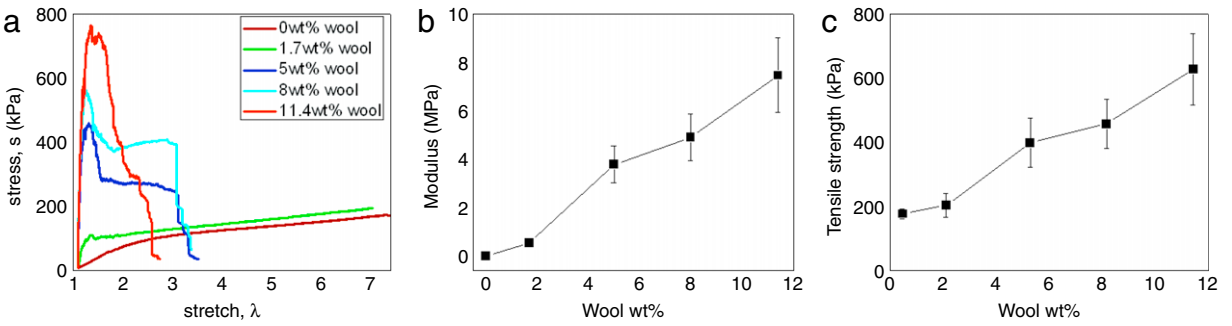

Fig. 6. Effect of fiber concentration. (a) Stress–stretch curves of hybrid gels with various fiber concentrations; (b) Modulus of hybrid gels with various fiber concentrations; (c) Tensile strength of hybrid gels with various fiber concentrations.

the arrangement of the fibers, and the behavior of the fiber/matrix interface. As a result of this diversity, composites with very distinct attributes can be fabricated using the same matrix material. For example, recently Lin et al. [12] reinforced the same hydrogel with highly aligned fibers of a stretchy thermoplastic polymer. A comparison between their composites and ours is interesting. Our composites have a stress–strain behavior where the stress first peaks and then drops to a plateau of constant stress. The plateau makes it possible to tailor the stress at which energy dissipation occurs. This behavior is distinctly different from the behavior reported by Lin et al., where no plateau was observed. In our composites, fiber sliding is an important aspect of the failure mechanism and frictional losses represent a significant fraction of the energy dissipated during failure. In the composites described by Lin et al., energy is dissipated mainly as a result of fiber fracture. Our composites can sustain much higher stresses than predicted based on the rule of mixtures for the individual components: there is a strong synergistic effect between the steel wool and the matrix material. The stress–strain curves of the composites reported by Lin et al., in contrast, follow the rule of mixtures.

Our results suggest that fiber-reinforced tough hydrogels may be useful in applications that require toughness, strength and stiffness—examples include materials for energy absorption, materials for tendon repair surgery, flexible electronics and sensors. The distinct stress–stretch behavior of our composites are ideal to use as energy absorbing materials, for instance, to soften the effect of an impact on a helmet [23]. Although the total energy dissipated by the composite is similar to the energy absorbed by the tough hydrogel when stretched to rupture, the level of stress during the deformation can be tailored by changing the fiber concentration, a distinct advantage over the unreinforced hydrogel. When designing an energy absorbing material for helmets, the material should absorb as much energy as possible, while limiting the maximum stress to the head to approximately 0.9 MPa to prevent injury [23,24]. The hydrogel composites have high energy absorption and a plateau stress that can be tailored to not exceed the maximum allowable value. For example, a 5 wt% composite has an energy absorption of approximately 0.6 MJ/m^3 and a plateau stress of 0.3 MPa; an 8 wt% composite has an energy absorption of 0.9 MJ/m^3 and a plateau stress of 0.4 MPa. These values compare favorably with commonly used energy absorbing materials such as expanded polystyrene, which has an energy absorption of 0.8 MJ/m^3 and a maximum stress in the range of 0.7–0.9 MPa [24].

Another possible application of hydrogel composites would be in tendon repair surgery, where reinforcing patches are used to help torn tendons heal. Current reinforcing patches are made from materials including porcine dermis, porcine intestine submucosa, or porous polyurethaneurea (Artelon®). Current tendon repair patches have an initial stiffness comparable to our composites and a higher stiffness at large strains. Despite advances in surgical techniques, the structural failure rate of these patches can be very high. Failure has been attributed mainly to sutures cutting through the reinforcing patches [25], which should not be an issue for the tough hydrogel. A fiber-reinforced tough hydrogel may serve as a potential reinforcement patch for suturing, although different biocompatible reinforcing fibers would need to be used.

Finally, one can also envision applications where electronics and living tissue are coupled using flexible and stretchable devices [26–29], an area that has gained much interest recently. These devices are used to probe the electrical activity near the surfaces of the heart, brain, or skin. Recent work includes embedding a 3D network of silicon nanowires with electronic circuitry into a soft gel matrix [30]. By integrating electrical sensors within the 3D scaffolds, cellular activities and physicochemical changes can be monitored. One can envision a similar approach to probe cells in a beating heart or to instill a sense of touch in a soft robotic hand. When electronics and biological tissues are coupled with flexible and stretchable devices, these devices need to be matched to the mechanical properties of the biological tissues. The hydrogel composites have stiffness values up to 10 MPa. By comparison, cartilage has a stiffness in the range of 6–15 MPa, while skin has a stiffness of 1–3 MPa [31]. The properties of the hydrogel composite can be optimized to the specific application by selecting the appropriate fiber material, orientation distribution, and volume fraction.

4. Conclusion

We have used brittle and tough hydrogel matrices to prepare random fiber-reinforced composites. Composites

that have a brittle matrix such as an alginate hydrogel fail by fibers cutting through the matrix. Composites based on tough alginate–polyacrylamide hybrid hydrogels, on the other hand, fail by debonding and sliding of the fibers, dissipating a significant amount of energy in the process. They can carry significantly more load than either matrix or the random fiber network. The combination of high strength, stiffness, and toughness, and the ability of sustaining large strains, along with easy method of synthesis, makes fiber-reinforced tough hydrogel composites good candidates for a range of applications.

Acknowledgments

This work was supported by the MRSEC (DMR-0820484) at Harvard University and by the National Science Foundation through grant CMMI-1404653. The authors are grateful to Prof. David J. Mooney for providing the Instron machine used in the mechanical testing.

References

[1] K.Y. Lee, D.J. Mooney, Hydrogels for tissue engineering, Chem. Rev. 101 (2001) 1869–1879.
[2] R. Langer, Drug delivery and targeting, Nature 392 (1998) 5–10.
[3] D.J. Beebe, J.S. Moore, J.M. Bauer, Q. Yu, R.H. Liu, C. Devadoss, B. Jo, Functional hydrogel structures for autonomous flow control inside microfluidic channels, Nature 404 (2000) 588–590.
[4] P. Calvert, Hydrogels for soft machines, Adv. Mater. 21 (2009) 743–756.
[5] J.P. Gong, Why are double network hydrogels so tough, Soft Matter 6 (2012) 2583–2590.
[6] X. Zhao, Multi-scale multi-mechanism design of tough hydrogels: building dissipation into stretchy network, Soft Matter 10 (2014) 672–687.
[7] R.F. Ker, The design of soft collagenous load-bearing tissues, J. Exp. Biol. 202 (1999) 3315–3324.
[8] C.-D. Young, J.-R. Wu, T.-L. Tsou, High-strength, ultra-thin and fiber-reinforced pHEMA artificial skin, Biomaterials 19 (1998) 1745–1752.
[9] F.T. Moutos, L.E. Freed, F. Guilak, A biomimetic three-dimensional woven composite scaffold for functional tissue engineering of cartilage, Nature Mater. 6 (2007) 162–167.
[10] A. Agrawal, N. Rahbar, P.D. Calvert, Strong fiber-reinforced hydrogel, Acta Biomater. 9 (2013) 5313–5318.
[11] I.-C. Liao, F.T. Moutos, B.T. Estes, X. Zhao, F. Guilak, Composite three-dimensional woven scaffolds with interpenetrating network hydrogels to create functional synthetic articular cartilage, Adv. Funct. Mater. 23 (2013) 5833–5839.
[12] S. Lin, C. Cao, Q. Wang, M. Gonzalez, J.E. Dolbow, X. Zhao, Design of stiff, tough and stretchy hydrogel composites via nanoscale hybrid crosslinking and macroscale fiber reinforcement, Soft Matter 10 (2014) 7519–7527.
[13] S.N. Bakarich, R. Gorkin III, M. Panhuis, G.M. Spinks, Three-dimensional printing fiber reinforced hydrogel composites, ACS Appl. Mater. Interfaces 6 (18) (2014) 15998–16006.
[14] J.P. Gong, Y. Katsuyama, T. Kurokawa, Y. Osada, Double-network hydrogels with extremely high mechanical strength, Adv. Mater. 15 (2003) 1155–1158.
[15] K. Haraguchi, T. Takehisa, Nanocomposite hydrogels: a unique organic–inorganic network structure with extraordinary mechanical, optical, and swelling/de-swelling properties, Adv. Mater. 14 (2002) 1120–1124.
[16] T. Huang, H. Xu, K. Jiao, L. Zhu, H.R. Brown, H. Wang, A novel hydrogel with high mechanical strength: a macromolecular microsphere composite hydrogel, Adv. Mater. 19 (2007) 1622–1626.
[17] K.J. Henderson, T.C. Zhou, K.J. Otim, K.R. Shull, Ionically cross-linked triblock copolymer hydrogels with high strength, Macromolecules 43 (2010) 6193–6201.
[18] J.-Y. Sun, X.H. Zhao, W.R.K. Illeperuma, O. Chaudhuri, K.H. Oh, D.J. Mooney, J.J. Vlassak, Z. Suo, Highly stretchable and tough hydrogels, Nature 489 (2012) 133–136.
[19] C. Gamonpilas, M.N. Charalambides, J.G. Williams, Determination of large deformation and fracture behavior of starch gels from conventional and wire cutting experiments, J. Mater. Sci. 44 (2009) 4976–4986.
[20] F. Baldi, F. Bibnotti, I. Peroni, S. Agnelli, T. Ricco, On the measurement of the fracture resistance of polyacrylamide hydrogels by wire cutting test, Polym. Test. 31 (2012) 455–465.
[21] A. Bentur, R. Cree, Cement reinforced with steel wool, Int. J. Cem. Compos. Lightweight Concrete 9 (1987) 217–223.
[22] L. Li, D.D.L. Chung, Electrical and mechanical properties of electrically conductive polyethersulfone composites, Composites 35 (1992) 215–223.
[23] N.J. Mills, A. Gilchrist, The effectiveness of foams in bicycle and motorcycle helmets, Accid. Anal. Prev. 23 (1991) 153–163.
[24] http://www.grantadesign.com/resources/materials/casestudies/helmet.htm.
[25] S. Chaudhury, C. Holland, M.S. Thompson, F. Vollrath, A.J. Carr, Tensile and shear mechanical properties of rotator cuff repair patches, J. Shoulder Elbow Surg. 21 (2012) 1168–1176.
[26] B.P. Timko, et al., Electrical recording from hearts with flexible nanowire device arrays, Nano Lett. 9 (2009) 914–918.
[27] J. Viventi, et al., Flexible, foldable, actively multiplexed, high-density electrode array for mapping brain activity *in vivo*, Nature Neurosci. 14 (2011) 1599–1605.
[28] D.-H. Kim, et al., Epidermal electronics, Science 333 (2011) 838–843.
[29] N. Lu, C. Lu, S. Yang, J. Rogers, Highly sensitive skin-mountable strain gauges based entirely on elastomers, Adv. Funct. Mater. 22 (2012) 4044–4050.
[30] B. Tian, J. Liu, T. Dvir, L. Jin, J.H. Tsui, Q. Qing, Z. Suo, R. Langer, D.S. Kohane, C.M. Lieber, Macroporous nanowire nanoelectronic scaffolds for synthetic tissues, Nature Mater. 11 (2012) 986–994.
[31] M.F. Ashby, The CES EduPack Database of Natural and Man-Made Materials, Granta Design, Cambridge, UK, 2008.